Fate of $\mathbb{CP}^{N-1}$ Fixed Points with q Monopoles

Matthew S. Block,[1] Roger G. Melko,[2] and Ribhu K. Kaul[1]

[1]*Department of Physics and Astronomy, University of Kentucky, Lexington, Kentucky 40506-0055, USA*
[2]*Department of Physics and Astronomy, University of Waterloo, Ontario N2L 3G1, Canada and Perimeter Institute for Theoretical Physics, Waterloo, Ontario N2L 2Y5, Canada*

(Received 1 July 2013; published 26 September 2013)

We present an extensive quantum Monte Carlo study of the Néel to valence-bond solid (VBS) phase transition on rectangular- and honeycomb-lattice SU(N) antiferromagnets in sign-problem-free models. We find that in contrast to the honeycomb lattice and previously studied square-lattice systems, on the rectangular lattice for small N, a first-order Néel-VBS transition is realized. On increasing $N \geq 4$, we observe that the transition becomes continuous and with the *same* universal exponents as found on the honeycomb and square lattices (studied here for $N = 5, 7, 10$), providing strong support for a deconfined quantum critical point. Combining our new results with previous numerical and analytical studies, we present a general phase diagram of the stability of $\mathbb{CP}^{N-1}$ fixed points with q monopoles.

DOI: 10.1103/PhysRevLett.111.137202 PACS numbers: 75.10.Jm, 64.70.Tg, 75.40.Cx, 75.40.Mg

The study of quantum critical points (QCPs) has seen a lot of excitement in both recent theoretical [1] and experimental work [2,3]. The most novel QCPs are those that do not have simple classical analogues in one higher dimension. One of the most prominent examples of such a QCP is the direct continuous "deconfined" critical point (DCP) between Néel and valence-bond solid (VBS) phases in bipartite SU(N) antiferromagnets [4]. Both states of matter are characterized by conventional broken symmetries, the Néel state by SU(N) symmetry breaking and the VBS by lattice symmetry breaking. A naive application of Landau theory would predict that since the two phases break distinct symmetries, a direct Néel-VBS transition cannot be continuous. However, by a subtle conspiracy of quantum interference and deconfinement, it has been shown that a continuous transition beyond the Landau paradigm can occur [5]. While the deconfined theory is by itself speculative (a "scenario"), the discovery of sign-problem-free models has allowed for unbiased tests by quantum Monte Carlo calculations of the theoretical proposal on large two-dimensional lattice models, in a way unprecedented for an exotic quantum critical phenomenon [6].

The speculative assumptions that underlie the DCP concept concern the existence and stability of certain critical fixed points. The DCP idea builds on the $\mathbb{CP}^{N-1}$ description of bipartite two-dimensional SU(N) quantum antiferromagnets [7]. The $\mathbb{CP}^{N-1}$ field theory consists of N complex scalars z_α interacting with a U(1) gauge field a_μ. Destructive interference from Berry phases results in the suppression of monopoles in a_μ unless they have a charge q [8]. A central result is that q in the simplest cases (of interest here) is equal to the degeneracy of the VBS phase [7], so the square lattice has $q = 4$, the honeycomb lattice has $q = 3$, and the rectangular lattice has $q = 2$. The discussion so far is on firm grounds. The two speculative ingredients that allow for a deconfined quantum critical point between Néel and VBS states in SU(N) antiferromagnets on lattices with q-fold degenerate VBS state are (1) the existence of a critical fixed point in the "noncompact" monopole-free $\mathbb{CP}^{N-1}$ theory [9] (this will be referred to as nc-$\mathbb{CP}^{N-1}$) and (2) the "dangerous irrelevance" of q-monopole insertions at the nc-$\mathbb{CP}^{N-1}$ fixed point. If these two conditions are met, the resulting "deconfined" renormalization group (RG) flow diagram [10] is as shown in Fig. 1(a).

The most extensive studies of deconfined criticality in microscopic models have focused on the case $N = 2$ and

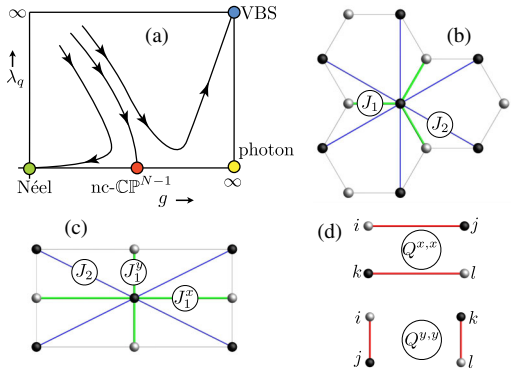

FIG. 1 (color online). (a) Deconfined RG flow diagram for SU(N) antiferromagnets with q-fold degenerate VBS phases, in the field theoretic space of monopole fugacity for q monopoles (λ_q) and the tuning parameter g of the critical point (see the text and Ref. [10] for details). In this work, we give a complete phase diagram in q-N space for which this RG flow diagram can be realized (see Table I). (b)–(d) Couplings of Eq. (1): (b) The honeycomb lattice with J_1 and J_2. (c) The rectangular lattice with J_1^x, J_1^y, and J_2. (d) The Q interaction shown is used here only on the rectangular systems. The A and B sublattices (black and white sites) have SU(N) spins transforming in the fundamental and conjugate to fundamental representations, respectively.

$q = 4$ [11–15] [i.e., the square lattice with SU(2) spins]. Other studies have tackled the cases $q = 4$, $2 \leq N \leq 12$ [16–19] [square lattice with SU(N) spins] and $N = 2$, $q = 3$ [20] [the honeycomb lattice with SU(2) spins]. The nature of the transition in the $q = \infty$ limit for $N = 2$ by studying the classical nc-$\mathbb{CP}^{N-1}$ model in three dimensions has been debated extensively [21–24]. We shall extend the studies of deconfined criticality by studying the case $q = 2$ (rectangular lattice) and $q = 3$ (honeycomb) for $N \leq 10$. Our main conclusions are as follows: We find clear evidence that the Néel-VBS transition on the rectangular lattice ($q = 2$) is first order for $N = 2$, 3 and continuous for $N \geq 4$. We find that the anomalous dimensions (η_N and η_V) for $N = 5$, 7, 10 are in agreement with each other on the rectangular lattices ($q = 2$), honeycomb lattices ($q = 3$), and square lattices ($q = 4$), all of which are consistent with the analytic $1/N$ expansion for the nc-$\mathbb{CP}^{N-1}$ model ($q = \infty$) (see Fig. 5). Finally, combining our new results with existing work, we suggest a general phase diagram for the values of N and q for which the deconfined RG flow in Fig. 1(a) is realized and a continuous deconfined Néel-VBS transition can occur (see Table I).

Model.—We consider bipartite SU(N) antiferromagnets in which the spins on the A sublattice transform under the fundamental representation of SU(N) while those on the B sublattice transform under the conjugate to the fundamental representation used fruitfully in both past analytic [25,26] and numerical [27,28] studies. Following previous work reviewed in detail in Ref. [6], we can construct sign-problem-free Hamiltonians that maintain the SU(N) symmetry from two operators, a projection operator $\mathcal{P}_{ij} = \sum_{\alpha,\beta=1}^{N} |\alpha\alpha\rangle_{ij}\langle\beta\beta|_{ij}$ (with i and j on opposite sublattices) and a permutation operator $\Pi_{ij} = \sum_{\alpha,\beta=1}^{N} |\alpha\beta\rangle_{ij} \times \langle\beta\alpha|_{ij}$ (with i and j on the same sublattice). The Hamiltonian we will study can be written in the following very general form:

$$H = -\sum_{i,j} \frac{J_1^{ij}}{N} \mathcal{P}_{ij} - \sum_{i,j} \frac{J_2^{ij}}{N} \Pi_{ij} - \sum_{\text{pl}} \frac{Q^{ij,kl}}{N^2} \mathcal{P}_{ij}\mathcal{P}_{kl}. \quad (1)$$

Illustrations of how each of the terms appears are shown in Figs. 1(b)–1(d). For small N, the J_1 only models are always Néel ordered, and for large N, they are always VBS ordered. To study the Néel-VBS transition at fixed N, we use the J_2 and Q terms. As studied previously, the J_2 interaction strengthens the Néel state by favoring ferromagnetic order on each of the sublattices [18], while the Q interaction favors the VBS phase by preferring the plaquettes to enter singlet states [11]. With the Hamiltonian so defined, we can study all the Néel-VBS phase transitions of interest, as we detail below. We shall study the model Hamiltonian using the unbiased and powerful stochastic series expansion quantum Monte Carlo method [29]. Details of the observables are provided in the Supplemental Material [30].

Rectangular lattice.—We begin by studying the phase transition between the Néel state and a $q =$ twofold degenerate VBS as a function of N. We study Eq. (1) on a rectangular lattice [see Fig. 1(b)], where the couplings are chosen to have rectangular symmetry, i.e., are invariant under translation in x and y but break the $\pi/2$ rotation symmetry that would be present on a square lattice. On such a lattice, the VBS state must be twofold degenerate, achieving $q = 2$ [31]. Specifically, we begin by taking $J_1^y = 0.8J_1^x$. For these couplings, the model is Néel ordered for $N \leq 4$ and VBS ordered for $N > 4$ (see the Supplemental Material [30] for details). To study the Néel-VBS transition for $N \leq 4$, we add a Q interaction (here, we use $Q^{y,y} = 0.8Q^{x,x}$) and tune the ratio $J_1^x/Q^{x,x}$. Remarkably, we find first-order transitions for $N = 2$, 3 (see Fig. 2) and a continuous transition for $N = 4$ (see the Supplemental Material [30]). For $N > 4$, we can study the Néel-VBS transition by introducing a J_2 coupling. For all $N > 4$, we find strong evidence for a continuous transition. A sample of our data for $N = 7$ is shown in Fig. 3 (additional data for $N = 5$, 10 are shown in the Supplemental Material [30]). Although we note that in principle our finding of a first-order transition cannot rule out a continuous transition in another model with the same q, N, it is natural to assume that the first-order transition observed for $q = 2$ is generic and results from the relevance of λ_2 for $N = 2$, 3. This assumption lends itself naturally to an interesting interpretation of our numerical observation that for $q = 2$, the transition is first order for $N = 2$, 3 and continuous for $N \geq 4$: in general, we expect that for a fixed q, the scaling dimension of the monopole operator

TABLE I. Table showing the inferred relevance (R) or irrelevance (I) of q monopoles at the nc-$\mathbb{CP}^{N-1}$ fixed point, which our current study has allowed us to complete. Numerical simulations of the Néel-VBS transition in the models discussed here only allow studies for $N \geq 2$. The entries with R correspond to an unstable fixed point and I to a stable fixed point that can then support the RG flow of Fig. 1(a). At some currently unknown critical value of $N > 10$, the $q = 1$ case switches from R to I.

$N = \infty$, $1/N$	I	I	I	I	$\cdots$	I	nc-$\mathbb{CP}^{N-1}$
$\cdots$							
$N = 10$	R	I	I	I		I	nc-$\mathbb{CP}^9$
$N = 9$	R	I	I	I		I	nc-$\mathbb{CP}^8$
$N = 8$	R	I	I	I		I	nc-$\mathbb{CP}^7$
$N = 7$	R	I	I	I		I	nc-$\mathbb{CP}^6$
$N = 6$	R	I	I	I		I	nc-$\mathbb{CP}^5$
$N = 5$	R	I	I	I		I	nc-$\mathbb{CP}^4$
$N = 4$	R	I	I	I		I	nc-$\mathbb{CP}^3$
$N = 3$	R	R	I	I		I	nc-$\mathbb{CP}^2$
$N = 2$	R	R	I	I		I	nc-$\mathbb{CP}^1$
$N = 1$	R	R	R	I		I	XY
$N = 0$	R	R	R	R		R	Photon
	$q = 1$	$q = 2$	$q = 3$	$q = 4$	$\cdots$	$q = \infty$	

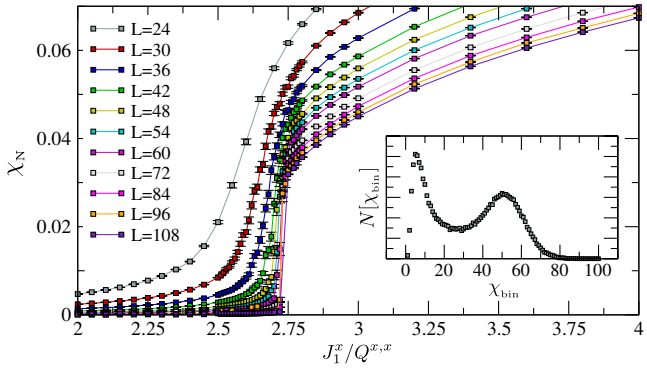

FIG. 2 (color online). First-order transition for $q = 2$ and $N = 3$ [rectangular lattice with SU(3) spins]. Magnetic susceptibility for SU(3) on the rectangular lattice. The sharp jump is indicative of a first-order transition. The inset shows a double-peaked histogram of data taken from a point in the middle of the transition ($J_1^x/Q^{x,x} = 2.71$) for $L = 48$, thus providing further evidence for a first-order transition. To accommodate the rectangular-lattice symmetry [41], we take a lattice with $L_x = 4L_y/3$; $L = L_y$ in our legend.

should increase as N increases [32]. What we have observed here then is that for $q = 2$, the scaling dimension is large enough to become irrelevant only when $N \geq 4$ [in agreement with the RG flow in Fig. 1(a)], but for $N = 2, 3$, the operator is a relevant perturbation [in contradiction to the RG flow shown in Fig. 1(a)] and thus drives the transition first order.

Honeycomb lattice.—Next, we study the case of a $q =$ threefold degenerate valence-bond solid phase. We can achieve this by studying our model [Eq. (1)] on the honeycomb lattice [see Fig. 1(a)]. The cases of SU(2), SU(3), and SU(4) have recently been studied [20,33], and the transition was shown to be continuous and is expected to remain continuous for larger N [32]. Our goal is to verify this expectation by studying the QCP for large N and extract η_N and η_V at the critical point for $N = 5$, 7, 10. Our starting point now is a J_1 only model on the nearest neighbors of a honeycomb lattice, which is VBS ordered for $N = 5$, 7, 10 (see the Supplemental Material [30] for a full study of the J_1 model as a function of N). To tune into the Néel state, we introduce a J_2 between second nearest neighbors on the honeycomb. We observe very good evidence for a continuous transition; a sample of our data for $N = 7$ is shown in Fig. 4.

Discussion.—In addition to the results already presented for SU(7), we have extracted η_N and η_V for $q = 2$, 3 and $N = 5$, 10. Figure 5 shows all of our results in comparison to previous data from the square-lattice study [18] and the analytic predictions [32,34,35]. Our procedure for extracting the critical exponents, as well as the values of the critical couplings, is detailed in the Supplemental Material [30]. We find that within the error bars of our

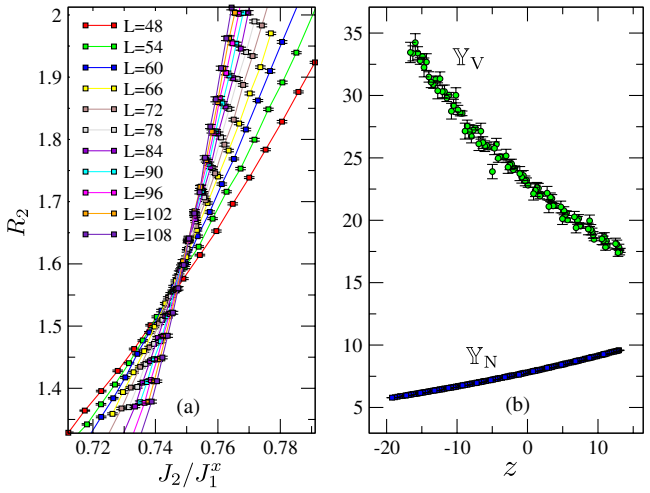

FIG. 3 (color online). Continuous transition for $q = 2$ and $N = 7$ [rectangular lattice with SU(7) spins]. (a) This panel shows the Binder ratio data. (b) Both the magnetic (blue squares) and VBS (green circles) susceptibility data. The data have been collapsed such that $\mathbb{Y}_N(z) = L^{1+\eta_N}\chi_N(z) + (a + bz)L^{-\omega}$ and $\mathbb{Y}_V(z) = L^{1+\eta_V}\chi_V(z)$ with $\eta_N = 0.639$, $a = 8.5$, $b = 0.1$, $\omega = 0.5$, and $\eta_V = 1.26$. Also, $z = [(g - g_c)/g_c]L^{1/\nu}$ with $g = J_2/J_1^x$, $g_c = 0.7552$, and $\nu = 0.69$. For the magnetic susceptibility, the following system sizes were used in the collapse: $L = 42$, 48, 54, 60, 66, 72, 78, 84, 90, 96, 102, 108. For the VBS susceptibility, the following system sizes were used in the collapse: $L = 36$, 42, 48, 54, 60, 66.

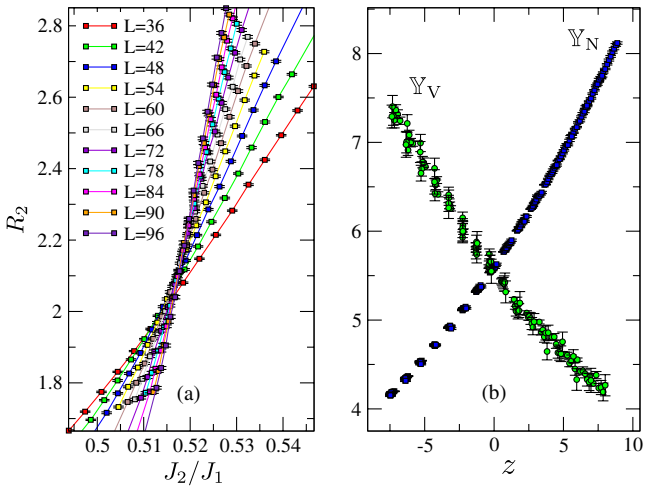

FIG. 4 (color online). Continuous transition for $q = 3$ and $N = 7$ [honeycomb lattice with SU(7) spins]. (a) The Binder ratio. (b) Both the magnetic (blue squares) and VBS (green circles) susceptibility data. The data have been collapsed such that $\mathbb{Y}_N(z) = L^{1+\eta_N}\chi_N(z) + (a + bz)L^{-\omega}$ and $\mathbb{Y}_V(z) = L^{1+\eta_V}\chi_V(z)$ with $\eta_N = 0.67$, $a = 20.0$, $b = 0.8$, $\omega = 1.0$, and $\eta_V = 1.41$. Also, $z = [(g - g_c)/g_c]L^{1/\nu}$ with $g = J_2/J_1$, $g_c = 0.5196$, and $\nu = 0.72$. For the magnetic susceptibility, the following system sizes were used in the collapse: $L = 36$, 42, 48, 54, 60, 66, 72, 78, 84, 90, 96. For the VBS susceptibility, the following system sizes were used in the collapse: $L = 18$, 24, 30, 36, 42, 48, 54. There are $2L^2$ lattice sites.

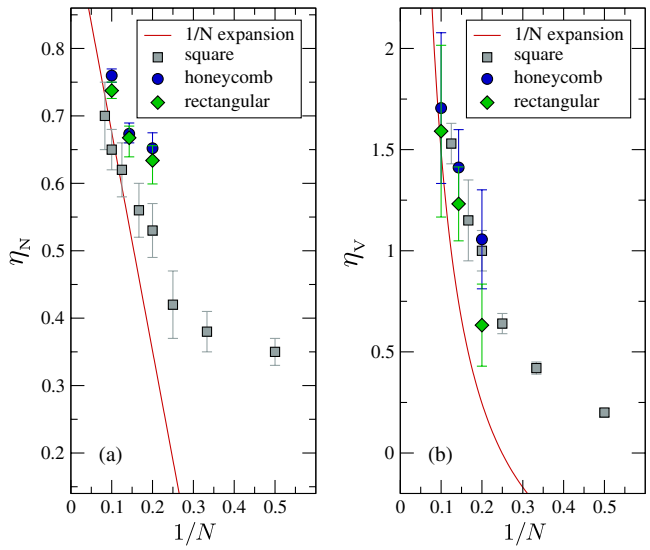

FIG. 5 (color online). Comparison of anomalous dimensions of Néel and VBS operators in the case of continuous transitions for $q = 2$, 3, and 4. (a) Anomalous dimension of the Néel order parameter as a function of $1/N$. (b) Anomalous dimension of the VBS order parameter as a function of $1/N$. The gray squares are the results of a previous square-lattice study ($q = 4$) [16,18]. The blue circles are new results from the honeycomb lattice ($q = 3$), and the green diamonds are new results from the rectangular lattice ($q = 2$). The red line is the $1/N$ expansion. The agreement of the new data with both the $q = 4$ data as well as the $1/N$ computation is striking.

calculation, the anomalous dimensions of the Néel and VBS order parameters are the same for rectangular, honeycomb, and square lattices, which is strong evidence for the fact that the phase transition in these three different cases is controlled by the same fixed point. This must mean that the lattice anisotropy is irrelevant for $N = 5$, 7, 10, which in the field theory language corresponds to the irrelevance of two-, three-, and fourfold monopoles at these fixed points [10]. In addition, we find that as N increases, the critical indices approach the value computed in the $1/N$ expansion in the nc-$\mathbb{CP}^{N-1}$ field theory, as shown in Fig. 5. This is evidence that the common critical point is indeed the nc-$\mathbb{CP}^{N-1}$ theory, as predicted by "deconfined criticality."

We now put our results in a broader context (see Table I and, for a more detailed discussion, the Supplemental Material [30]). Since the critical theory of the SU(N) Néel to q-fold degenerate VBS transition is described by the $\mathbb{CP}^{N-1}$ theory with q monopoles, we can think of our numerical simulations of antiferromagnets as a way to learn about the $\mathbb{CP}^{N-1}$ theory with q monopoles. The nc-$\mathbb{CP}^{N-1}$ fixed point is known to exist analytically at large N [36] and for $N = 1$ [37] (for $N = 0$, there are no matter fields and one has a stable photon phase). We shall take the point of view that by continuity, it exists for all N; this is the rightmost column of Table I (we note here that the case $N = 2$ has been debated in the literature [21–24]).

We can now ask whether q monopoles are relevant (R) or irrelevant (I) at the nc-$\mathbb{CP}^{N-1}$ fixed point. Past analytic and field theoretic works have addressed the question for $N = 0$ [38], $N = 1$ [37], and $N = \infty$ [32]. The column $q = 1$ has recently been addressed in simulations of loop models [39] and bilayer SU(N) antiferromagnets [40]. The column $q = 4$ has been addressed by studying the critical point of the square-lattice Néel-VBS transition [18]. Here, we have provided the final piece of the puzzle by studying the $q = 2$ and $q = 3$ cases (see Ref. [20] for a study of $q = 3$, $N = 2$), where we have explicitly seen the change from a first-order to a continuous transition as N is increased for $q = 2$. The rest of the table can be filled out by making the reasonable assumption that once an entry is I, it will stay I for increasing q or N. It is expected that the $q = 1$ column will switch from R to I at some large finite value of N; this value has not been accessed in numerical simulations currently.

We gratefully acknowledge helpful discussions with M. Fisher and A. Sandvik. The research reported here was supported in part by NSF DMR-1056536 (M. S. B. and R. K. K.) and the Natural Sciences and Engineering Research Council of Canada (R. G. M.)

[1] C. Xu, Int. J. Mod. Phys. B **26**, 1230007 (2012).
[2] R. Coldea, D. A. Tennant, E. M. Wheeler, E. Wawrzynska, D. Prabhakaran, M. Telling, K. Habicht, P. Smeibidl, and K. Kiefer, Science **327**, 177 (2010).
[3] X. Zhang, C.-L. Hung, S.-K. Tung, and C. Chin, Science **335**, 1070 (2012).
[4] T. Senthil, A. Vishwanath, L. Balents, S. Sachdev, and M. Fisher, Science **303**, 1490 (2004).
[5] T. Senthil, L. Balents, S. Sachdev, A. Vishwanath, and M. P. A. Fisher, Phys. Rev. B **70**, 144407 (2004).
[6] R. K. Kaul, R. G. Melko, and A. W. Sandvik, Annu. Rev. Condens. Matter Phys. **4**, 179 (2013).
[7] N. Read and S. Sachdev, Phys. Rev. B **42**, 4568 (1990).
[8] F. D. M. Haldane, Phys. Rev. Lett. **61**, 1029 (1988).
[9] O. I. Motrunich and A. Vishwanath, Phys. Rev. B **70**, 075104 (2004).
[10] T. Senthil, L. Balents, S. Sachdev, A. Vishwanath, and M. P. A. Fisher, J. Phys. Soc. Jpn. **74**, 1 (2005).
[11] A. W. Sandvik, Phys. Rev. Lett. **98**, 227202 (2007).
[12] R. G. Melko and R. K. Kaul, Phys. Rev. Lett. **100**, 017203 (2008).
[13] F. Jiang, M. Nyfeler, S. Chandrasekharan, and U. Wiese, J. Stat. Mech. (2008) P02009.
[14] A. W. Sandvik, Phys. Rev. Lett. **104**, 177201 (2010).
[15] A. Banerjee, K. Damle, and F. Alet, Phys. Rev. B **82**, 155139 (2010).
[16] J. Lou, A. W. Sandvik, and N. Kawashima, Phys. Rev. B **80**, 180414 (2009).
[17] R. K. Kaul, Phys. Rev. B **84**, 054407 (2011).
[18] R. K. Kaul and A. W. Sandvik, Phys. Rev. Lett. **108**, 137201 (2012).
[19] A. Banerjee, K. Damle, and F. Alet, Phys. Rev. B **83**, 235111 (2011).

[20] S. Pujari, K. Damle, and F. Alet, Phys. Rev. Lett. **111**, 087203 (2013).
[21] O. I. Motrunich and A. Vishwanath, arXiv:0805.1494.
[22] A. B. Kuklov, M. Matsumoto, N. V. Prokof'ev, B. V. Svistunov, and M. Troyer, Phys. Rev. Lett. **101**, 050405 (2008).
[23] F. S. Nogueira, S. Kragset, and A. Sudbø, Phys. Rev. B **76**, 220403 (2007).
[24] K. Chen, Y. Huang, Y. Deng, A. B. Kuklov, N. V. Prokof'ev, and B. V. Svistunov, Phys. Rev. Lett. **110**, 185701 (2013).
[25] I. Affleck, Phys. Rev. Lett. **54**, 966 (1985).
[26] N. Read and S. Sachdev, Phys. Rev. Lett. **62**, 1694 (1989).
[27] K. Harada, N. Kawashima, and M. Troyer, Phys. Rev. Lett. **90**, 117203 (2003).
[28] K. S. D. Beach, F. Alet, M. Mambrini, and S. Capponi, Phys. Rev. B **80**, 184401 (2009).
[29] A. W. Sandvik, AIP Conf. Proc. **1297**, 135 (2010).
[30] See Supplemental Material at http://link.aps.org/supplemental/10.1103/PhysRevLett.111.137202 for more details and additional numerical results.
[31] K. Harada, N. Kawashima, and M. Troyer, J. Phys. Soc. Jpn. **76**, 013703 (2007).
[32] G. Murthy and S. Sachdev, Nucl. Phys. **B344**, 557 (1990).
[33] K. Harada, T. Suzuki, T. Okubo, H. Matsuo, J. Lou, H. Watanabe, S. Todo, and N. Kawashima, arXiv:1307.0501.
[34] M. A. Metlitski, M. Hermele, T. Senthil, and M. P. A. Fisher, Phys. Rev. B **78**, 214418 (2008).
[35] R. K. Kaul and S. Sachdev, Phys. Rev. B **77**, 155105 (2008).
[36] B. I. Halperin, T. C. Lubensky, and S.-k. Ma, Phys. Rev. Lett. **32**, 292 (1974).
[37] C. Dasgupta and B. I. Halperin, Phys. Rev. Lett. **47**, 1556 (1981).
[38] A. M. Polyakov, *Gauge Fields and Strings* (Harwood Academic, Chur, Switzerland, 1987).
[39] A. Nahum, J. T. Chalker, P. Serna, M. Ortuño, and A. M. Somoza, Phys. Rev. Lett. **107**, 110601 (2011).
[40] R. K. Kaul, Phys. Rev. B **85**, 180411 (2012).
[41] A. W. Sandvik, Phys. Rev. Lett. **83**, 3069 (1999).